EUROPEAN ORGANIZATION FOR NUCLEAR RESEARCH

A COMPARATIVE STUDY OF THE DISSOCIATION OF PROTONS INTO LOW-MASS $p\pi^+\pi^-$ SYSTEMS IN COHERENT AND INCOHERENT PROTON-NUCLEUS COLLISIONS AT 18.6 GeV/c

P.C. Bruton[1], T. Ekelöf[2,3], S.M. Fisher[1], P. Grafström[2,3], E. Hagberg[2,3], D.C. Imrie[1], S. Jonsson[2], S. Kullander[2] and J. Nassalski[1,4]

ABSTRACT

A decay angular moments analysis has been performed on 8500 $p\pi^+\pi^-$ events produced by the interaction of high-energy protons with nuclear targets. The analysis was carried out separately for the low-t, coherent events and the high-t, incoherent events. The moments of the two samples show significant differences and possible reasons for such differences are discussed.

Geneva - 10 December 1976
(Submitted to Nuclear Physics)

---

1 University College, London, England

2 The Gustav Werner Institute, Uppsala, Sweden

3 CERN, Geneva, Switzerland

4 Institute of Nuclear Research, Warsaw, Poland.

1. INTRODUCTION

One of the basic properties of coherent production on nuclear targets is that isospin-one exchange, $I_x = 1$, is strongly suppressed with respect to $I_x = 0$ exchange, in comparison with production on nucleons[1]. One can enhance the fraction of coherent events from a nuclear target by selecting events from the region of small momentum transfers, where the differential cross-section is characterized by the nuclear form factor. In the region of larger momentum transfers, on the other hand, incoherent production dominates and the $I_x = 1$ exchange is not suppressed. In this paper we describe some results of a counter experiment in which both coherent and incoherent processes were recorded with approximately equal acceptances. One of the aims of the experiment was to make a comparative study of coherent and incoherent dissociation of protons into low-mass $p\pi^+\pi^-$ states ($m_{p\pi^+\pi^-} \leq 2$ GeV) in proton--nucleus scattering at 18.6 GeV/c.

In an experiment studying low-mass $p\pi^+\pi^-$ production in proton-proton interactions at 12 GeV/c and 24 GeV/c incident momenta[2], it has been observed that the cross-sections for some of the produced spin states of the $p\pi^+\pi^-$ system decrease with increasing incident momentum. Such spin states are most probably produced through the exchange of secondary Regge trajectories. If some of these trajectories have $I_x \neq 0$, then the corresponding $p\pi^+\pi^-$ states will be suppressed in the coherent event sample of our data as compared with the incoherent sample. However, the composition of the two samples can also be modified by differences in the momentum-transfer dependence of the elementary production amplitudes for the various states, which somewhat complicates the interpretation of the data. On the other hand, comparing coherent and incoherent events produced in the same measurement ensures that effects due to apparatus inefficiencies and incomplete acceptance are largely eliminated in the comparison.

The apparatus and analysis procedure of the present experiment have been described elsewhere[3]. 53,000 triggers were recorded with a C target, 32,000 with an Al target, 24,000 with an Ag target and 16,000 with a U target. From these, a total of 8,500 events have been selected with $p\pi^+\pi^-$ effective masses below 2 GeV.

In order to separate an enhanced sample of coherent events, a cut in t' was applied at a certain value t'_{lim}. This value was derived for each target using the formula

$$t'_{lim} = -0.22\ (GeV/c)^2 \cdot A^{-2/3}\ ,$$

where $t' = t - t_{min}$ is approximated by the perpendicular three-momentum transfer squared, p_T^2, and A is the atomic number of the nucleus. The constant $-0.22\ (GeV/c)^2$ was chosen empirically to ensure that, for each target, the cut was approximately at the break between the coherent nuclear slope and the incoherent nucleon slope. This cut divided the sample of 8500 events into two parts of approximately equal statistics.

In fig. 1 the $d\sigma/dt$ distributions obtained with the C, Al and Ag targets are shown. The curves are fitted with double exponentials in t', the expressions of which are given in the figure caption. The values of t'_{lim} are indicated by an arrow in each distribution. In this paper, events with $|t'|$ less than $|t'_{lim}|$ will be referred to as "coherent", and events with $|t'|$ greater than $|t'_{lim}|$ as "incoherent".

2. EFFECTIVE MASS DISTRIBUTIONS

The $p\pi^+\pi^-$ effective mass distributions are independent of the target nucleus to within the statistical precision of the experiment and, in the analysis described below, we have combined events from all targets. Figure 2 shows the $p\pi^+\pi^-$ effective mass distributions, corrected for acceptance, for the coherent and incoherent event samples, separately. The over-all mass acceptance in the range up to 2 GeV is 34%, varying from 64% at the lower limit to 22% at 2 GeV. The acceptance in t' varies from 32% to 23% over the $|t'|$ range of 0.0-0.5 $(GeV/c)^{-2}$.

Both $p\pi^+\pi^-$ mass distributions are qualitatively similar to the spectrum obtained from proton targets. They show two enhancements centred at 1.45 and 1.7 GeV. During the last ten years a great effort[2,4-6] has been made to associate these enhancements with resonances discovered by phase-shift analysis of formation

experiments. It now seems to be clear that no simple assignment can be made and that the correct interpretation must be in terms of the interference of several partial waves[2].

The 1.7 GeV enhancement is less pronounced in the coherent (fig. 2a) than in the incoherent sample (fig. 2b), comparing with the 1.45 enhancement. A tempting explanation of the difference between the two spectra would be that the 1.7 GeV region of the incoherent mass distribution contains a greater I = $^3/_2$ component than 1.45 GeV region. However, experiments on hydrogen[4,5] have shown that the slope of the differential cross-section of the production on nucleons is steeper at low mass values than at high. Such an effect could account for the differences between the low-t, coherent, and high-t, incoherent, mass distributions in fig. 2.

The two t' distributions, obtained with the carbon target in the $p\pi^+\pi^-$ mass ranges 1.35-1.55 GeV and 1.6-1.8 GeV, were fitted separately with expressions containing two exponentials in t'. The values obtained for the exponential slope parameter of the nuclear coherent peak are 81 ± 14 $(GeV/c)^{-2}$ in the 1.35-1.55 GeV mass range and 64 ± 16 $(GeV/c)^{-2}$ in the 1.6-1.8 GeV mass range. The corresponding distributions, obtained from measurements with a hydrogen target, have been fitted with a single exponential in the low-t region, yielding slope parameters of around 14 $(GeV/c)^{-2}$ in the 1.35-1.55 GeV region and around 6 $(GeV/c)^{-2}$ in the 1.6-1.8 GeV region[4,5]. In the impulse approximation, the slope parameter of the nuclear coherent peak is equal to the sum of the slope parameters of the nuclear form factor and of the elementary, nucleonic amplitude. The difference in the two slope parameters above, obtained from the fits to the nuclear coherent peak, is consistent with this hypothesis. It is thus likely that the major difference between the two mass spectra in fig. 2 are due to the variation of the elementary slope with the $p\pi^+\pi^-$ mass as mentioned above.

The mass distributions of the three subsystems $p\pi^+$, $p\pi^-$ and $\pi^+\pi^-$ are shown for the two event samples separately in figs. 3, 4 and 5. The incoherent distributions show the same features as those obtained with proton targets, i.e. a very prominent Δ^{++} signal at 1.2 GeV in the $p\pi^+$ mass spectrum, a much weaker Δ^0 signal

at the same mass value in the $p\pi^-$ spectrum, and a broad, smooth $\pi^+\pi^-$ spectrum. The coherent distributions show the same features. However, in the coherent $\pi^+\pi^-$ spectrum there is some indication of a peak near the ρ mass, implying that the coherently produced $p\pi^+\pi^-$ system has a tendency to decay via the $p\rho$ intermediate state. There is no such indication in the incoherent $\pi^+\pi^-$ spectrum, nor in data obtained with a proton target[2].

3. ANGULAR DISTRIBUTIONS AND ACCEPTANCE CALCULATIONS

In order to obtain information on the spin composition of the two $p\pi^+\pi^-$ mass enhancements, an angular analysis has been performed. The distributions of the polar angle, β_i, of the normal to the $p\pi^+\pi^-$ decay plane and of the polar angle, θ_i, of the direction of motion of the $p\pi^+$ system, both measured in the $p\pi^+\pi^-$ rest frame, have been studied. The subscript i is either s or t and indicates that the z-axis in the $p\pi^+\pi^-$ rest frame has been chosen to correspond to the s- or t-channel helicity frames, respectively. In the former, the z-axis is opposite to the direction of the recoiling target particle; in the latter it is in the direction of the incoming proton.

The acceptance correction was carried out in two steps. First each physical event was rotated in azimuth around the beam direction and the acceptance fraction determined. The event was then assigned a geometrical weight equal to the reciprocal of this acceptance fraction.

In the second step, the event distributions were corrected for regions of phase space for which the acceptance fraction was zero. Monte Carlo events were generated according to a model with sequential two-body decays, which has the same correlated distribution in the masses of the $p\pi^+\pi^-$ and $p\pi^+$ systems and the same t' distribution as the experimental data had after the first step of acceptance corrections. The centre-of-mass distributions of the $p\pi^+\pi^- \to (p\pi^+) + \pi^-$ and $p\pi^+ \to p + \pi^+$ decay angles were assumed to be isotropic. The distributions of those Monte Carlo events for which the acceptance fraction was zero were then used to correct the input mass and t' distributions of the Monte Carlo program, and the

whole procedure was repeated in an iterative manner. The method proved to be convergent and the calculation was stopped when the distributions produced by two successive iterations differed by less than the statistical errors. The corrections to the angular distributions obtained in this way were, typically, 20%.

In order to investigate if this procedure was significantly dependent on the shape of the decay angular distributions, the calculations were repeated using a series of different functions for the decay distributions. The functions used were power series in the cosine of the decay angles and powers up to six were tried. It was found that the average correction varies between 15% and 25%, depending on the shape assumed, a negligible variation in view of the statistical precision of the data. The corrections obtained using the isotropic decays were found to be good averages of the corrections evaluated with other angular distributions and the final data were therefore corrected using isotropic decay angular distributions in the Monte Carlo program.

Figures 6 and 7 show the cos β_t and cos β_s distributions for the $p\pi^+\pi^-$ mass bins 1.45 ± 0.1 GeV and 1.7 ± 0.1 GeV, respectively. The coherent and incoherent event samples are shown separately. Figures 8 and 9 give the corresponding plots for cos θ_t and cos θ_s. In fig. 10 are shown the distributions of the cosine of the decay angle of the proton in the decay $(p\pi^+) \rightarrow p + \pi^+$ measured in the $p\pi^+$ centre of mass.

An attempt was made to fit these angular distributions to expressions[7] that follow from the hypothesis that only one spin state is present. The result of these fits was that both the expressions assuming pure spin $^3/_2$ and those assuming pure spin $^5/_2$ fitted the data reasonably well. There were no significant differences between the coherent and the incoherent event samples in this respect. However, the hypothesis of a single dominant state of spin $^1/_2$ could be ruled out for both samples. The strong assumption about the presence of only one spin state, which has to be made using this method, constitutes a considerable limitation. In order to make a more unprejudiced analysis of the angular distributions a moments analysis has been performed.

4. MOMENTS ANALYSIS OF THE ANGULAR DISTRIBUTIONS

The normalized moments $\langle Y_L^0 \rangle$ of the angular distributions have been calculated as the integral from -1.0 to +1.0 of the product of the spherical harmonic function $Y_\ell^{m=0}(z)$ and the measured cos θ_i and cos β_i distributions. The normalization is such that $\langle Y_0^0 \rangle = 1/\sqrt{4\pi} \approx 0.28$.

In figs. 11a and 11b are shown the moments of cos β_t and cos β_s, respectively, over the mass range 1.4 to 1.85 GeV for the coherent and incoherent event samples. Two signals are seen in the L = 2 moment of the coherent sample, one around 1.5 GeV and the other around 1.7 GeV. These signals are absent in the incoherent sample which, however, shows some signal at the lower end of the mass range. In the other moments, no strong signals are visible. A weak signal may be present at 1.7 GeV in the L = 6 moment of β_t.

The corresponding plots for the moments of θ_t and θ_s are shown in figs. 12a and 12b. The coherent sample again shows non-zero values for the L = 2 moment in the 1.5 GeV and 1.7 GeV mass regions. The incoherent sample shows no strong signals in the s-channel. In the t-channel, however, the L = 2 moment is different from zero at the same mass values as the coherent L = 2 moment. At higher even L values, L = 4 and L = 6, non-zero moments are seen in the coherent sample around 1.7 GeV. Also the odd moments, L = 1, L = 3, and L = 5, are non-zero indicating the presence of several interfering waves. The incoherent sample shows no stronger deviation from zero in the s-channel at any L. In the t-channel, however, the high mass moments are all non-zero. A peculiarity of the moments between L = 3 and L = 6 is that they appear to be comparatively narrow in mass. The same phenomenon, i.e. narrow peaks for the L > 2 moments in the mass region 1.7-1.8 GeV has been observed in proton dissociation into $p\pi$ at 14 GeV/c [5]. Evidence for a narrow peak in this mass region has also been found in other experiments as noted in Ref. 5. In our case this signal is only visible in θ_t moments of the incoherent sample.

5. CONCLUSIONS

We have studied the dissociation of protons into low-mass $p\pi^+\pi^-$ states on nuclear targets for two regions in four-momentum transfer squared: one low-t region, with mostly coherently produced events, and one high-t region, with incoherent events.

The $p\pi^+\pi^-$ mass distributions are different for the two regions. Within the statistical precision of the experiment, this difference can be accounted for by the observed mass dependence of the exponential slope of the elementary nucleon diffraction dissociation cross-sections. In the mass spectrum of the $\pi^+\pi^-$ subsystem there is some indication that part of the coherently produced $p\pi^+\pi^-$ system decays via the $p\rho$ intermediate state. There is no such indication in the incoherent case.

A moments analysis of the decay angles of the produced $p\pi^+\pi^-$ system has given the following results:

i) Using the normal to the decay plane as analyser in the s- and t-channel helicity frames, L = 2 moments were found in the coherent data around mass values of 1.5 GeV and 1.7 GeV. Corresponding moments could not be found in the incoherent data.

ii) Using the direction of motion of the $p\pi^+$ system as analyser, L = 2 moments were found above 1.5 GeV for the coherent data in both the s- and t-channel frames. For the incoherent data L = 2 moments were only observed in the t-channel frame. Above 1.6 GeV higher moments from L = 3 to L = 6 were found in the coherent event sample, indicating several interfering higher spin states. In the incoherent sample, a narrower peak in the 1.7-1.8 GeV region was observed in the t-channel for the same moments L = 3 to L = 6. Such a narrow structure has also been reported elsewhere[5].

In the 1.5 GeV mass region only the L = 2 moment is non-zero, which is compatible with the presence of a system with spin $J = {}^3/_2$. The many higher moments present above 1.6 GeV indicate the presence of several partial waves of different parity and it is probable that one of the interfering states has a spin higher

than $3/2$, i.e. $5/2$ or possibly $7/2$. Results from an evaluation of data[2] obtained with a hydrogen target, in which enhancements are seen at the same $p\pi^+\pi^-$ mass values as in our data, indicate that an important fraction of the events in both mass peaks is in the $3/2^-$ spin state and that the remaining fraction of the lower mass peak is $1/2^+$ and that of the higher $1/2^+$ and $5/2^+$. The presence of these states in both the coherent and the incoherent part of our data, obtained with nuclear targets, is certainly possible. However, the moments analysis shows that there are significant differences in the distribution of the angular momentum states between the low-t, coherent event sample and the high-t, incoherent event sample.

There are several phenomena that can contribute to such differences, one being that the coherent mechanism suppresses the $I \neq 1/2$ component of the produced system in the low-t region. The contribution of particle states with $I \neq 1/2$ and definite spin will therefore only appear in the incoherent moments. Another reason for differences is that the production amplitudes for the various spin-parity states have different t-dependences. It has been concluded from data[2] obtained with hydrogen targets that there are differences between the exponential slope parameters of the various states produced and this will thus cause differences in the contribution of these states to the low-t and high-t samples.

The detailed explanation of the differences between the angular distributions in the two t' regions is beyond the scope of this experiment. However, it seems likely that further high-statistics experiments with nuclear targets measuring the angular distributions of both coherently and incoherently produced mass systems could be of value in trying to disentangle the nature of the low-mass states obtained in high-energy proton dissociation.

This experiment has been carried out at CERN using the 28 GeV Proton Synchrotron, with financial support from CERN, The Swedish Atomic Research Council, and the Science Research Council of the United Kingdom. We would like to thank the CERN-Munich group for having put their spectrometer at our disposal. It is a great pleasure to thank our experimental colleagues, A.J. Herz, F.F. Heymann and G.J. Lush, for their help in the data-taking phase of the experiment.

REFERENCES

1) R.J. Glauber, "Theory of high-energy hadron-nucleus collisions" *in* High-Energy Physics and Nuclear Structure (Plenum Press, New York, 1970), p. 207.
H.H. Bingham, Proc. of Topical Seminar on Interactions of Elementary Particles with Nuclei, Trieste, 1970 (Eds. G. Bellini et al.), (INFN, Trieste, 1970), p. 37.

2) V. Blobel et al., Nuclear Phys. B97 (1975) 201.

3) P. Bruton et al., Phys. Letters 59B (1975) 490.

4) H. Johnstad et al., Nuclear Phys. B42 (1972) 558.

5) J. Ballam and V. Chaloupka, "Study of proton diffraction in $\pi^{\pm}$p collisions at 14 GeV/c", paper 1260/A1 143, submitted to the Tbilisi Conference on High-Energy Physics, 1976.

6) J.I. Rhode et al., Phys. Rev. 187 (1969) 1844.
J.G. Rushbrooke et al., Phys. Rev. 40 (1971) 3273.

7) S.M. Berman and M. Jacob, Phys. Rev. 139 (1969) 1844.

Figure captions

Fig. 1 : The distributions of the differential cross-section, integrated over all masses, obtained with the C, Al and Ag targets. The arrows indicate the t'_{lim} values for each case. The curves are the following double exponentials obtained in fits to the data:

(C) $(130 \pm 30) \times [\exp(67 \pm 13) \times t' + (0.29 \pm 0.09) \times$
$\times \exp(10.1 \pm 0.7) \times t'] \text{ mb/(GeV/c)}^2$.

(Al) $(510 \pm 110) \times [\exp(132 \pm 21) \times t' + (0.13 \pm 0.03) \times$
$\times \exp(11.0 \pm 0.3) \times t'] \text{ mb/(GeV/c)}^2$.

(Ag) $(1200 \pm 300) \times [\exp(247 \pm 56) \times t' + (0.15 \pm 0.04) \times$
$\times \exp(12.4 \pm 0.2) \times t'] \text{ mb/(GeV/c)}^2$.

Fig. 2 : Mass spectra of the $p\pi^+\pi^-$ system for (a) the low-t, coherent and (b) the high-t, incoherent event samples.

Fig. 3 : Mass spectra of the $p\pi^+$ subsystem for (a) the coherent and (b) the incoherent $p\pi^+\pi^-$ events.

Fig. 4 : Mass spectra of the $p\pi^-$ subsystem for (a) the coherent and (b) the incoherent $p\pi^+\pi^-$ events.

Fig. 5 : Mass spectra of the $\pi^+\pi^-$ subsystem for (a) the coherent and (b) the incoherent $p\pi^+\pi^-$ events.

Fig. 6 : Distributions of the cosine of the polar angle β of the normal to the $p\pi^+\pi^-$ decay plane in the $p\pi^+\pi^-$ mass bin 1.35-1.55 GeV: (a) in the t-channel helicity frame and (b) in the s-channel frame. The upper plots are for the low-t, coherent events and the lower ones for the high-t, incoherent events.

Fig. 7 : The same as fig. 6 but for the mass bin 1.6-1.8 GeV.

Fig. 8 : The same as fig. 6 except that the angle is the polar angle θ of the $p\pi^+$ direction of motion.

Fig. 9 : The same as fig. 6 except that the angle is the polar angle of the $p\pi^+$ direction of motion θ and that the mass bin is 1.6-1.8 GeV.

Fig. 10 : The cosine of the polar angle of the direction of motion of the proton in the $p\pi^+$ centre of mass in the $p\pi^+$ mass bin 1.1-1.3 GeV: (a) for the $p\pi^+\pi^-$ mass bin 1.35-1.55 GeV, and (b) for the $p\pi^+\pi^-$ mass bin 1.6-1.8 GeV. The upper plots are for the low-t, coherent events and the lower ones for the high-t, incoherent events.

Fig. 11 : The spherical harmonic moments, $\langle Y_L^0 \rangle$, of the normal to the decay plane as functions of the $p\pi^+\pi^-$ mass from 1.40 to 1.85 GeV: (a) in the t-channel and (b) in the s-channel. In each case the left figure is for the low-t, coherent events and the right one for the high-t, incoherent events.

Fig. 12 : The same as fig. 11 but for the direction of motion of the $p\pi^+$ system.

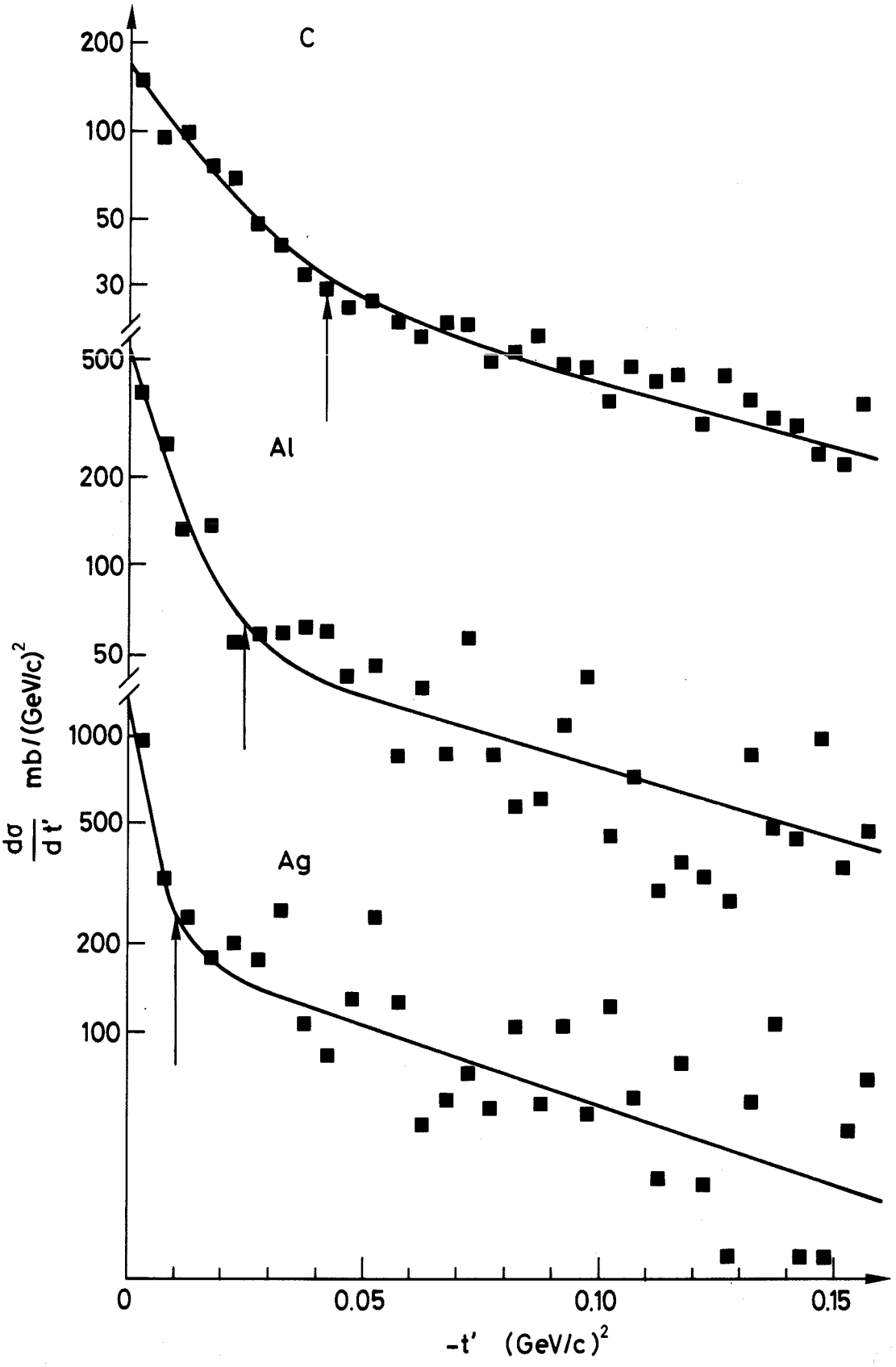
C
Al
Ag
200
100
50
30
500
200
100
50
1000
500
200
100
0
0.05
0.10
0.15
$\frac{d\sigma}{dt'}$ mb/(GeV/c)^2
-t' (GeV/c)^2

Fig. 1

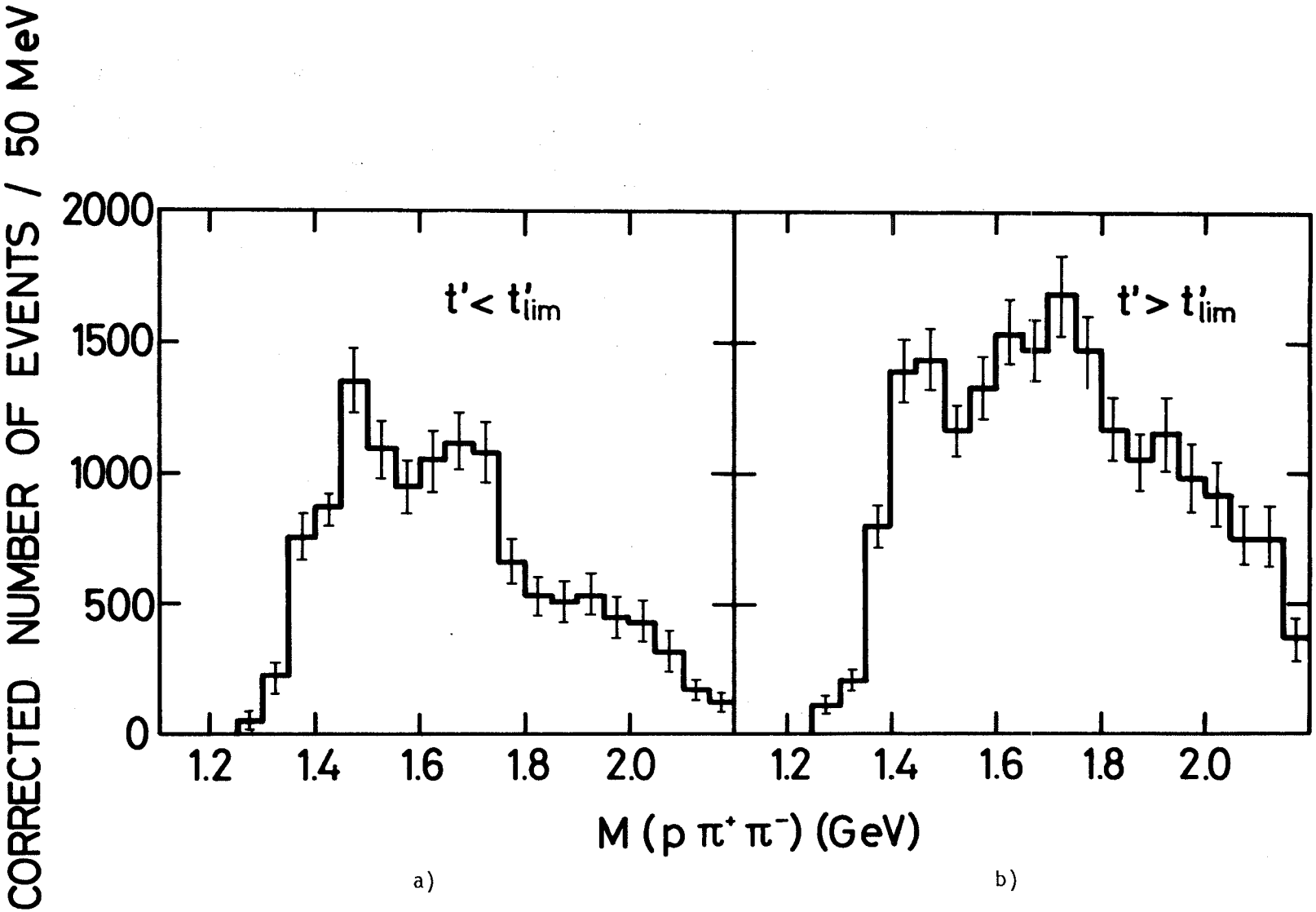
CORRECTED NUMBER OF EVENTS / 50 MeV
2000
1500
1000
500
0
t' < t'lim
t' > t'lim
1.2
1.4
1.6
1.8
2.0
M (p π⁺ π⁻) (GeV)
a)
b)

Fig. 2

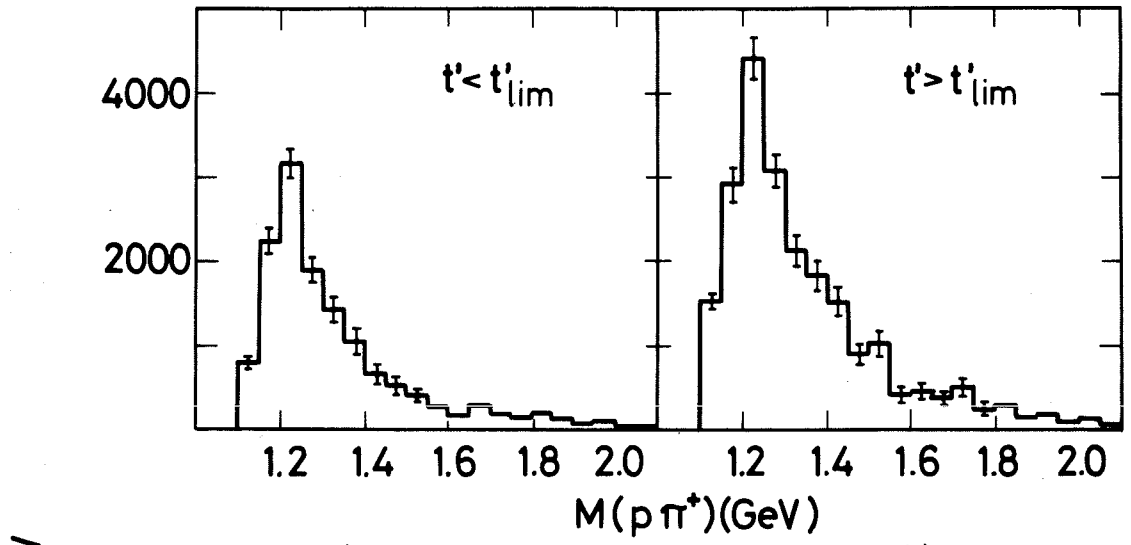

a) b)

Fig. 3

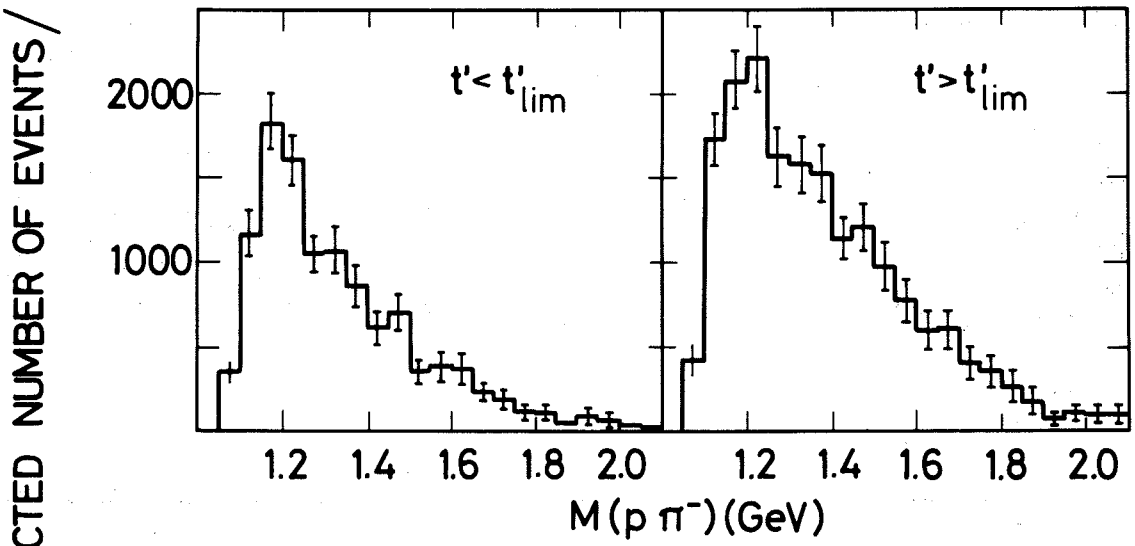

a) b)

Fig. 4

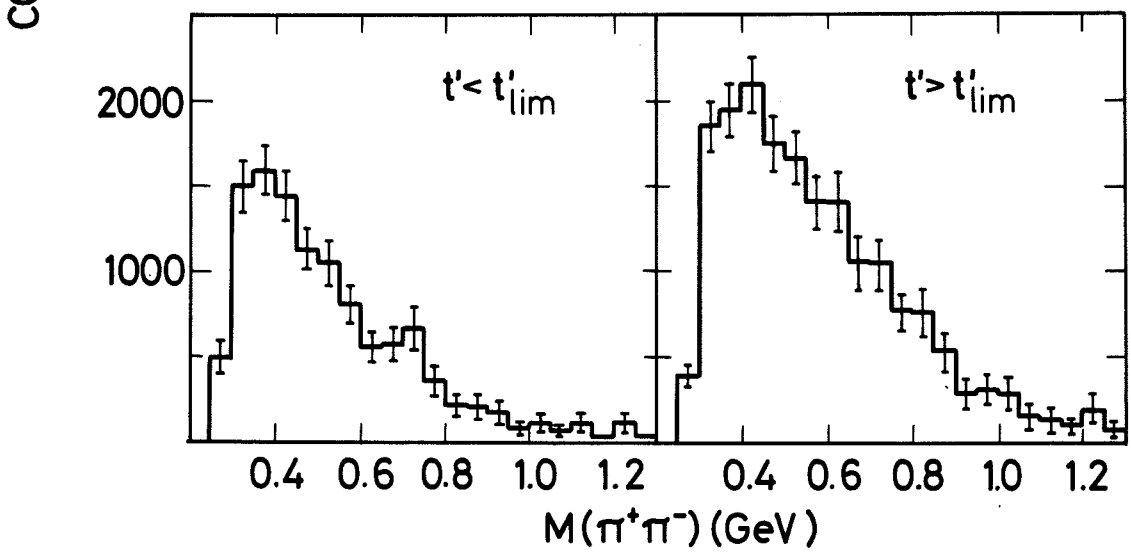

a) b)

Fig. 5

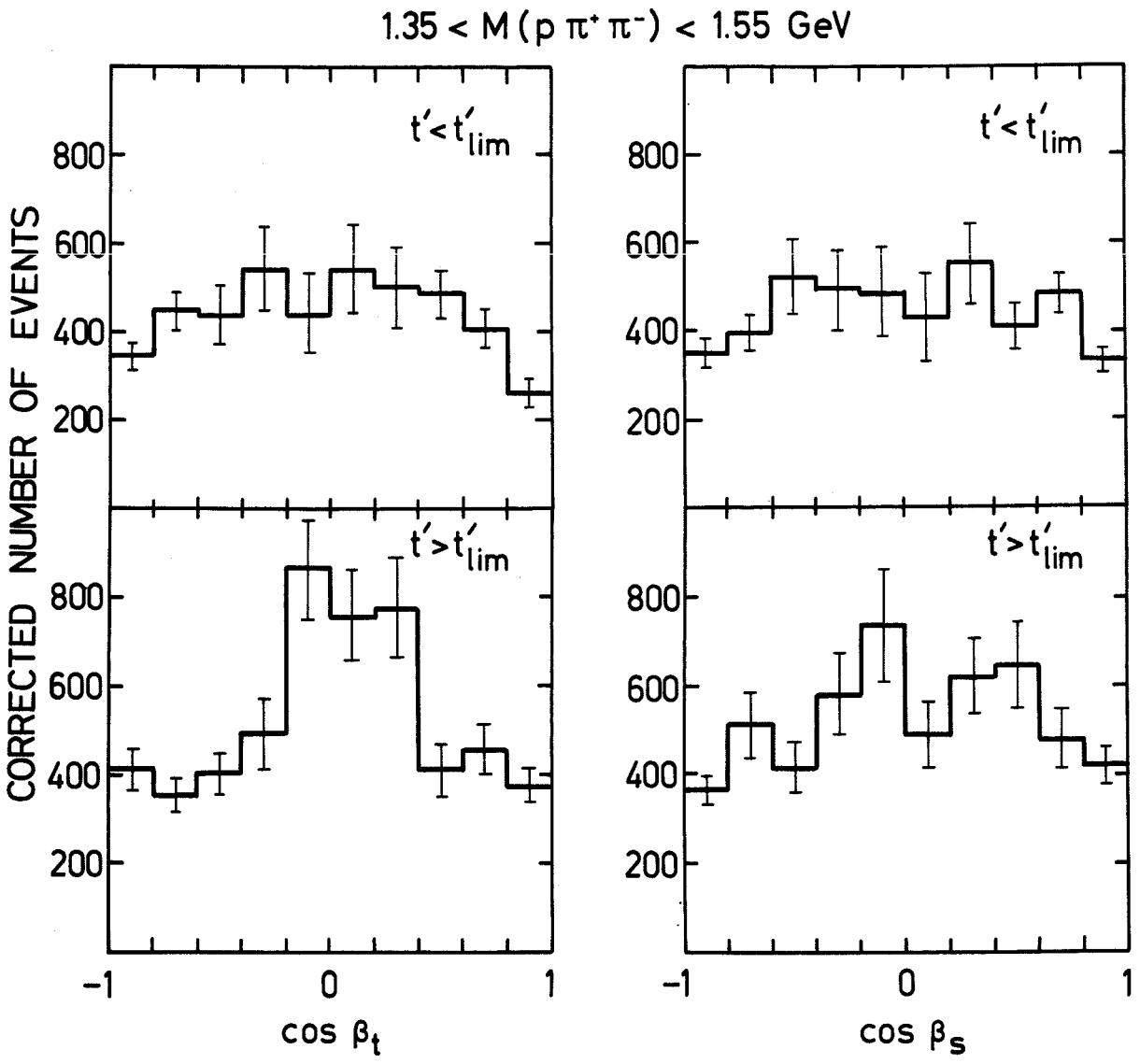
1.35 < M (p π⁺ π⁻) < 1.55 GeV
CORRECTED NUMBER OF EVENTS
t'<t'lim
t'>t'lim
800
600
400
200
-1
0
1
cos βt
cos βs
a)
b)

Fig. 6

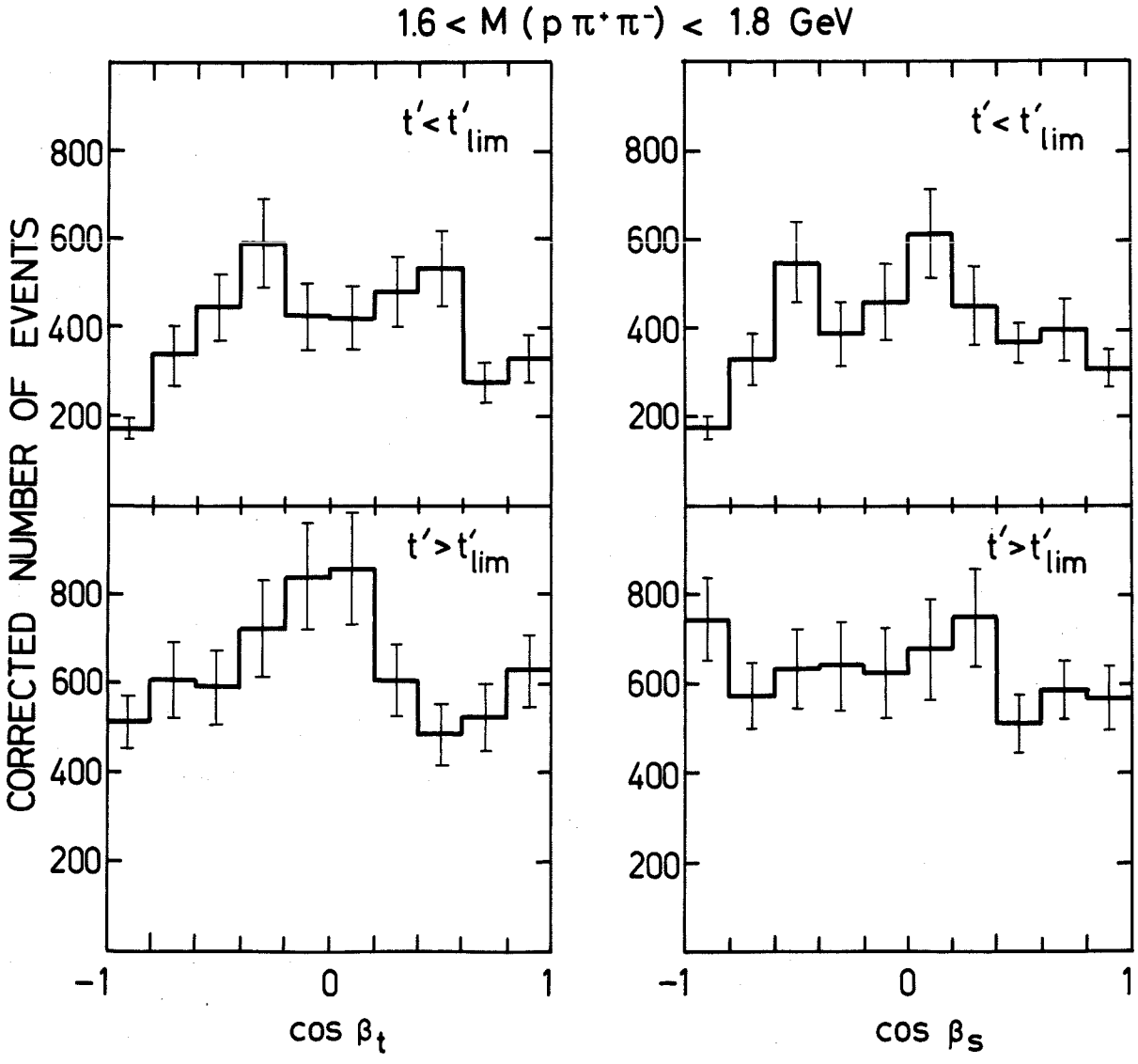
1.6 < M (p π⁺ π⁻) < 1.8 GeV
t′< t′lim
t′> t′lim
CORRECTED NUMBER OF EVENTS
800
600
400
200
−1
0
1
cos βt
cos βs
a)
b)

Fig. 7

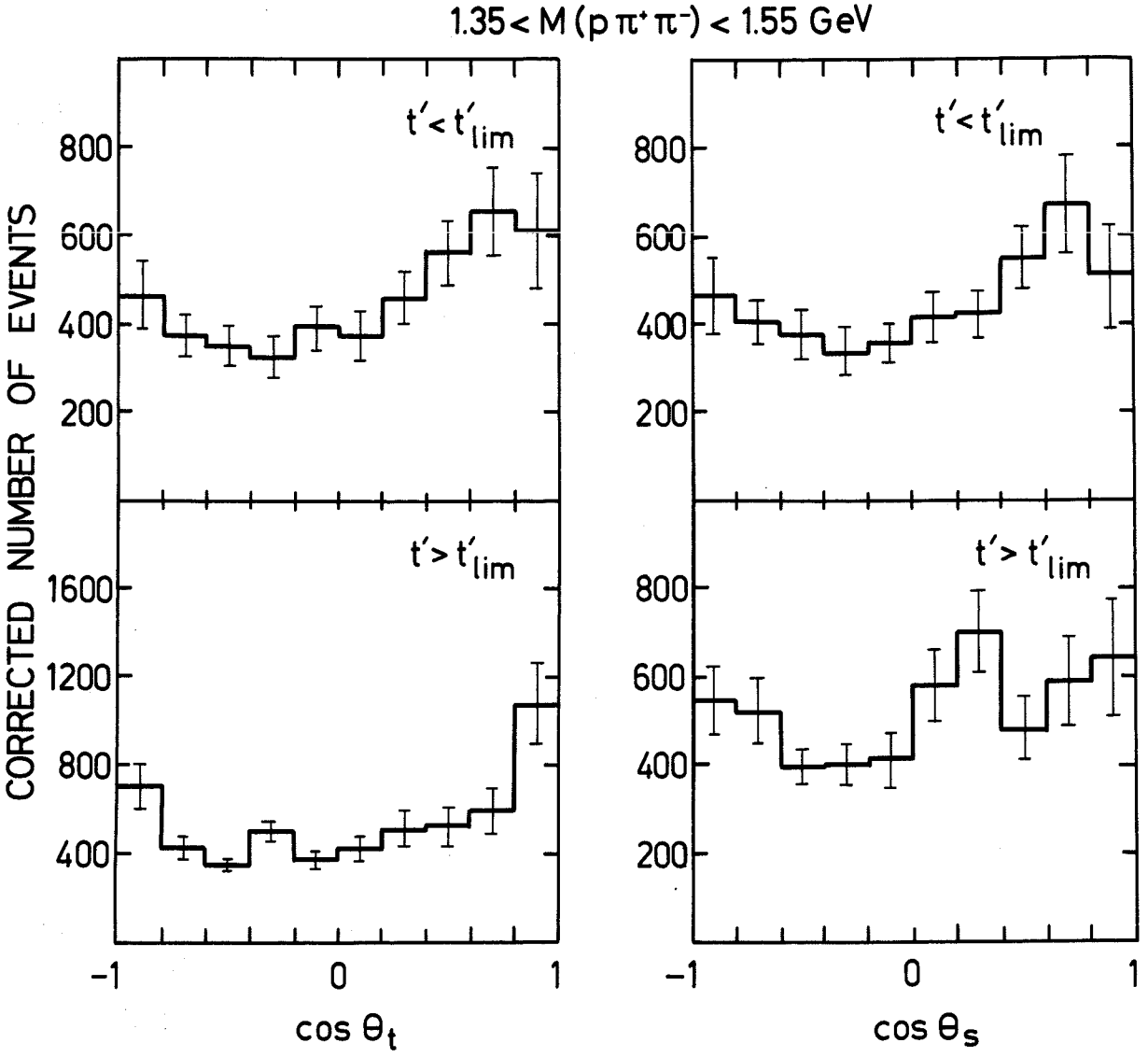
1.35 < M (p π⁺ π⁻) < 1.55 GeV
CORRECTED NUMBER OF EVENTS
t' < t'lim
t' > t'lim
800
600
400
200
1600
1200
800
400
-1
0
1
cos θt
cos θs
a)
b)

Fig. 8

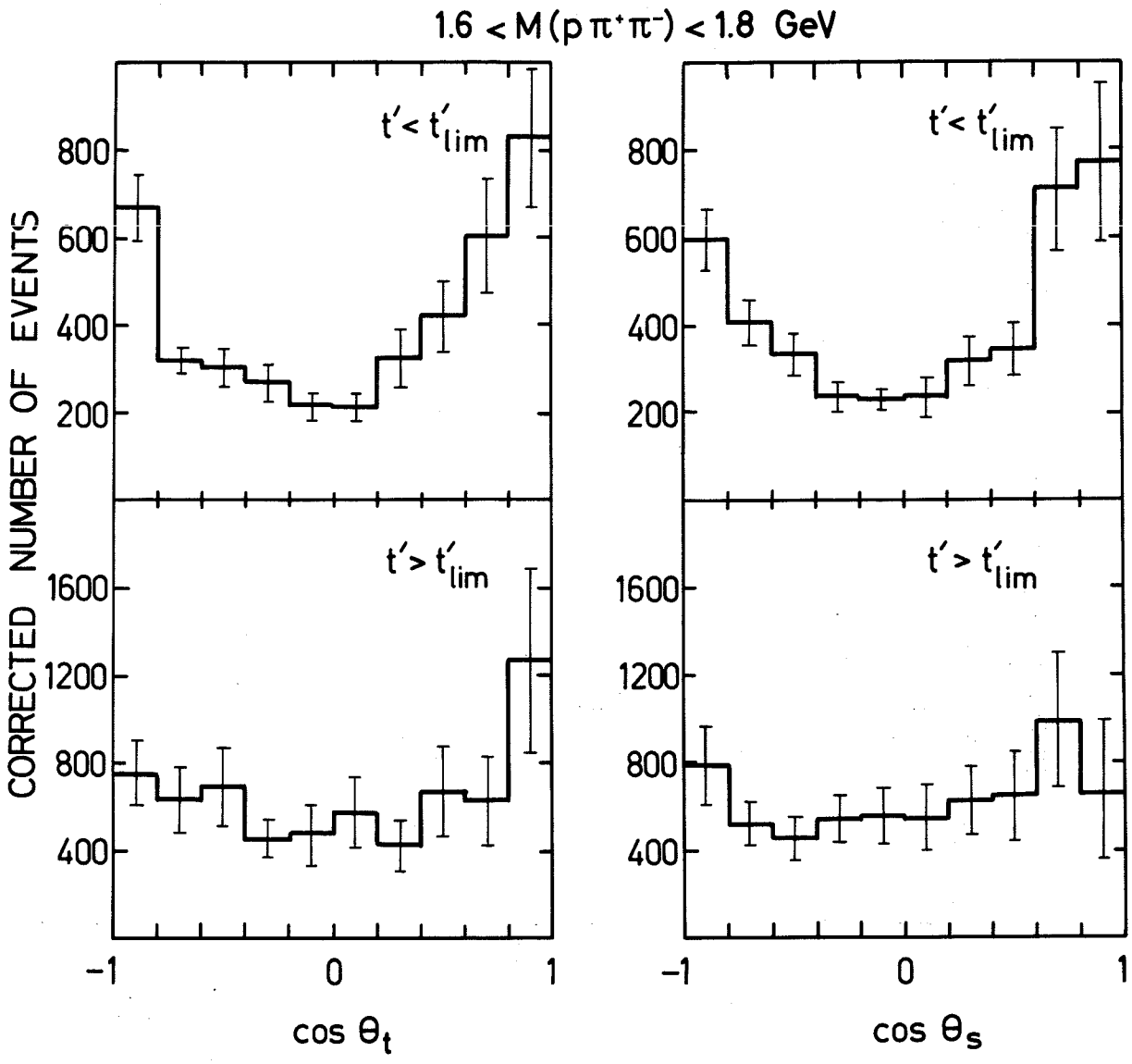
1.6 < M(p π⁺ π⁻) < 1.8 GeV
CORRECTED NUMBER OF EVENTS
t' < t'lim
t' > t'lim
800
600
400
200
1600
1200
800
400
-1
0
1
cos θt
cos θs
a)
b)

Fig. 9

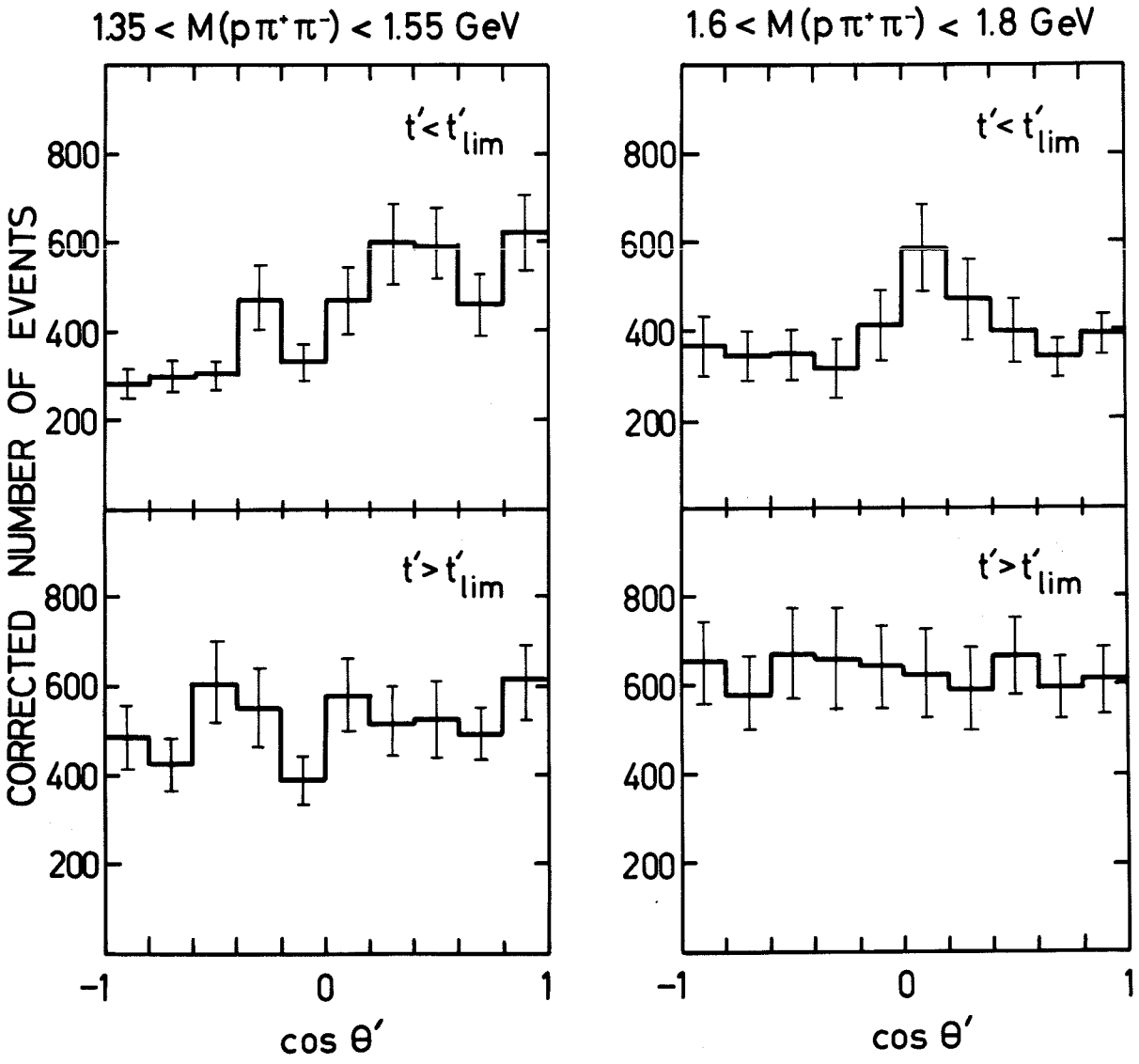
1.35 < M(pπ⁺π⁻) < 1.55 GeV
1.6 < M(pπ⁺π⁻) < 1.8 GeV
t'< t'lim
t'> t'lim
CORRECTED NUMBER OF EVENTS
800
600
400
200
-1
0
1
cos θ'
a)
b)

Fig. 10

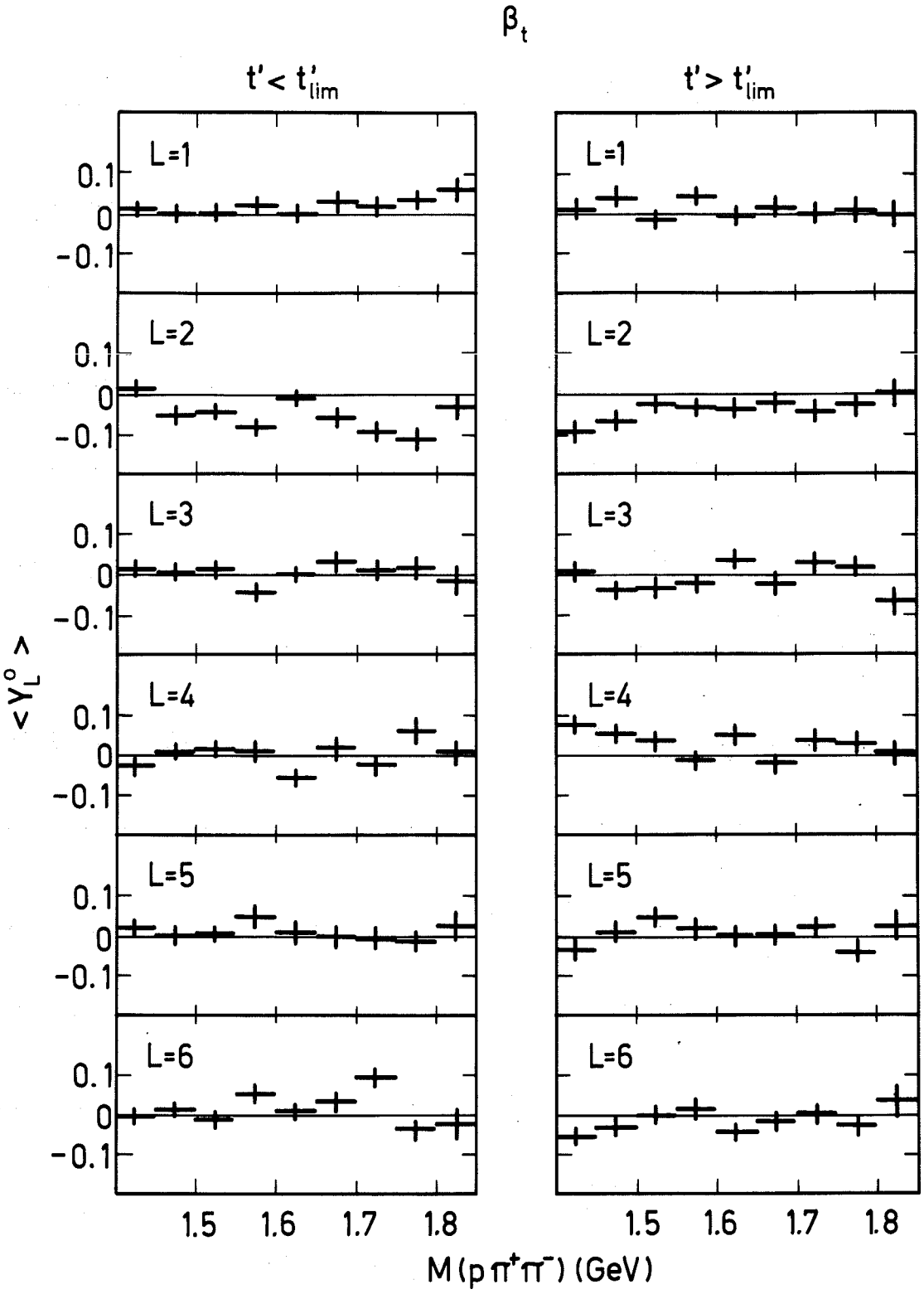
β_t
$t' < t'_{lim}$
$t' > t'_{lim}$
L=1
L=2
L=3
L=4
L=5
L=6
0.1
0
-0.1
$\langle Y_L^0 \rangle$
1.5
1.6
1.7
1.8
$M(p\pi^+\pi^-)$ (GeV)

Fig. 11a

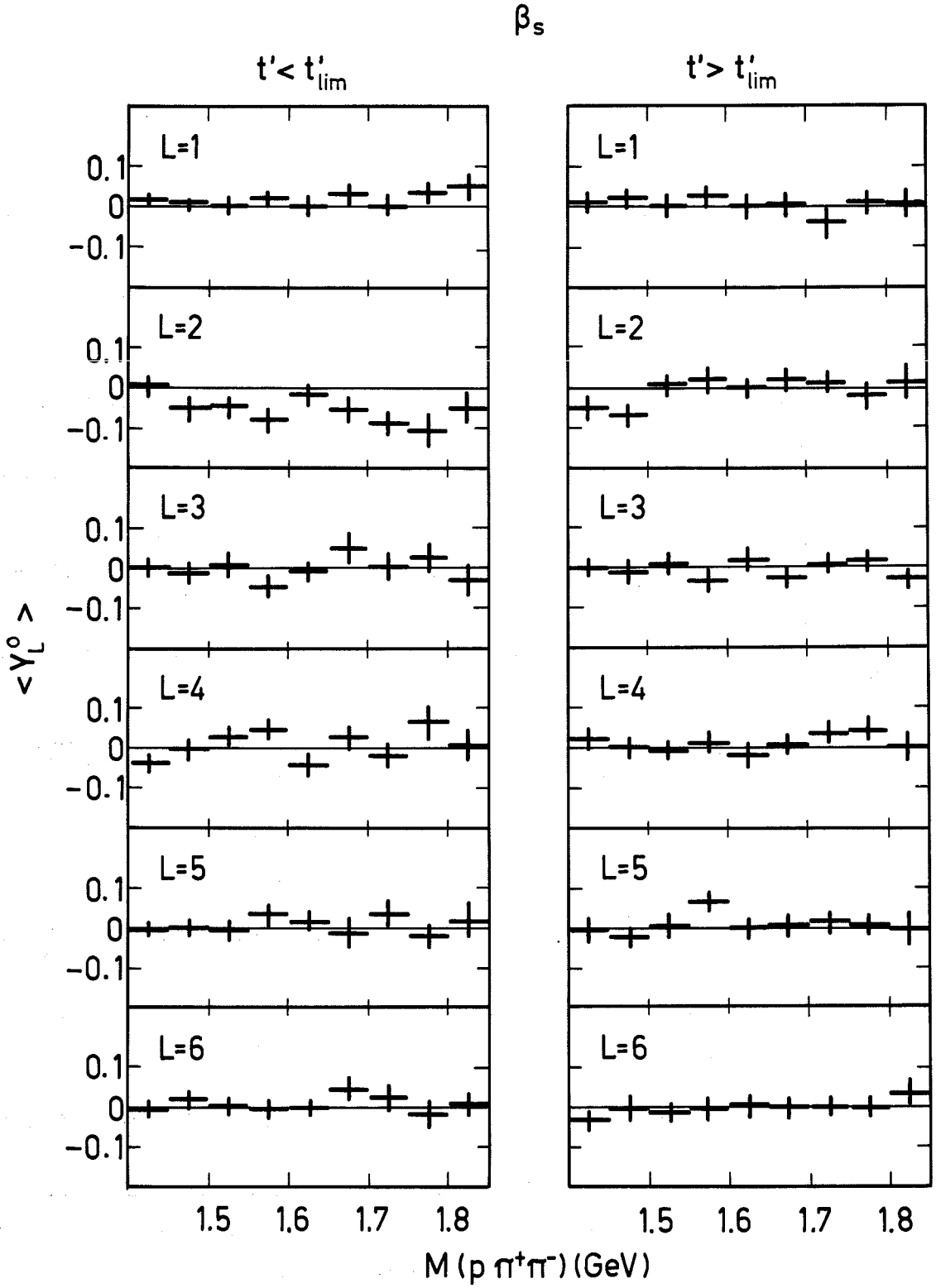
β_s
$t' < t'_{lim}$
$t' > t'_{lim}$
L=1
L=2
L=3
L=4
L=5
L=6
0.1
0
-0.1
$\langle Y_L^0 \rangle$
1.5
1.6
1.7
1.8
M (p $\pi^+\pi^-$) (GeV)

Fig. 11b

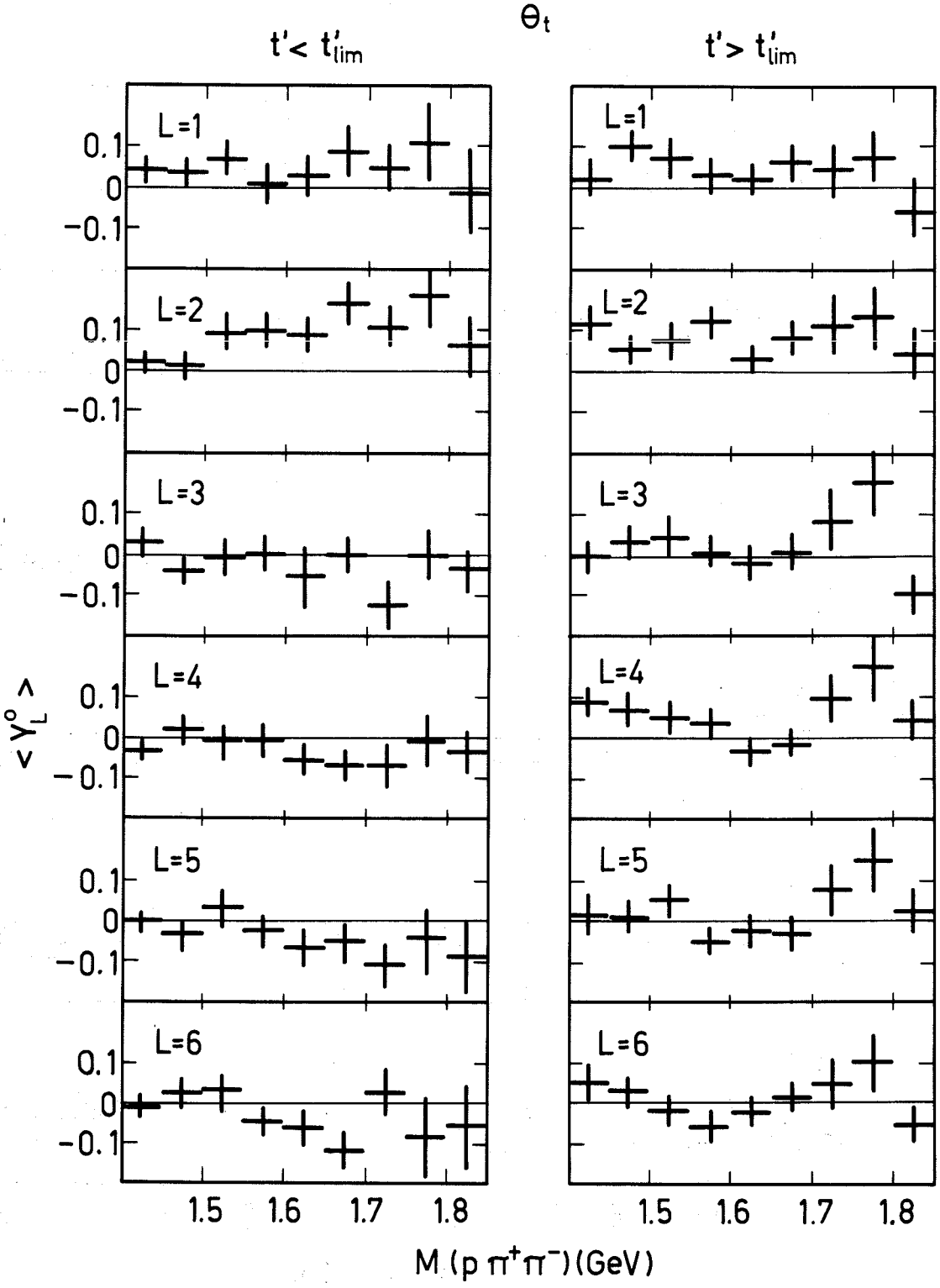
Θ_t
t'< t'lim
t'> t'lim
L=1
L=2
L=3
L=4
L=5
L=6
0.1
0
-0.1
$\langle Y_L^0 \rangle$
1.5
1.6
1.7
1.8
M (p π⁺π⁻) (GeV)

Fig. 12a

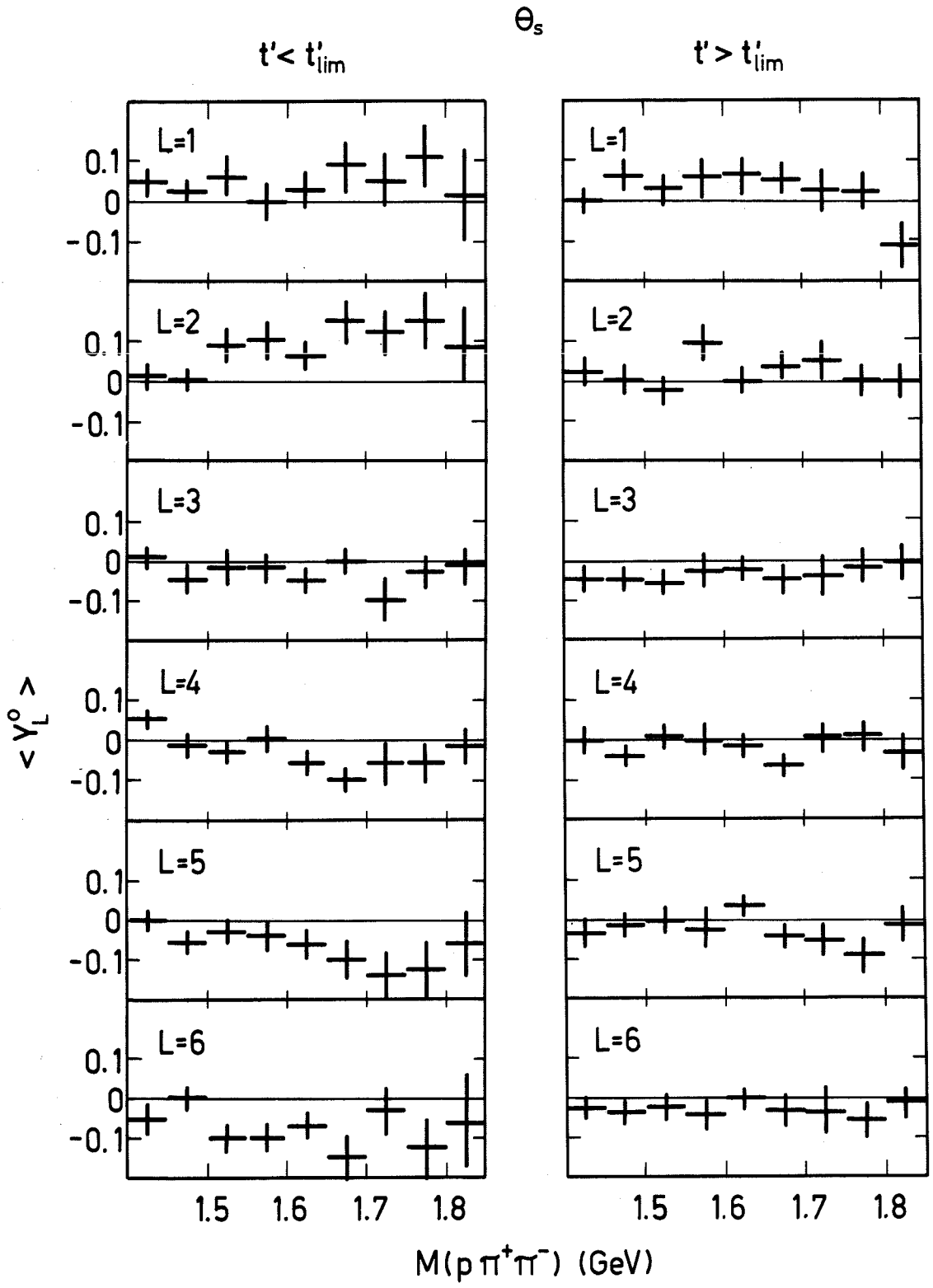
Θ_s
$t' < t'_{lim}$
$t' > t'_{lim}$
L=1
L=2
L=3
L=4
L=5
L=6
0.1
0
-0.1
$\langle Y_L^0 \rangle$
1.5
1.6
1.7
1.8
$M(p\pi^+\pi^-)$ (GeV)

Fig. 12b